Constructing 3D layered energetic metal-organic framework with strong stacking interactions of hydrogen-bridged rings: the way to insensitive high energy complex

Xiang Chen,[a] *Zhaoqi Guo,*[a] *Cong Zhang,*[a] *Rong Gao,*[b] *Jianguo Zhang*[c] and *Haixia Ma**[a]

[a] School of Chemical Engineering, Northwest University, Xi'an 710069, Shaanxi, P. R. China

[b] College of Chemistry and Materials Science, Northwest University, Xi'an 710069, Shaanxi, P. R. China

[c] State Key Laboratory of Explosion Science and Technology, Beijing Institute of Technology, Beijing 100081, P. R. China

Table of Contents

1. Selected bond lengths, bond angles and hydrogen bonds for 1 and 2.

Table S1 Hydrogen bonds present in **1**

D–H···A	d(D–H)/Å	d(H–A)/Å	d(D–A)/Å	D–H–A/°
O4–H4A···O2^{iv}	0.86(2)	2.50(5)	3.025(5)	120(4)
O4–H4A···O3^{v}	0.86(2)	2.25(3)	3.005(6)	147(5)
O4–H4B···N4	0.85(2)	2.29(4)	2.998(5)	141(5)
N3–H3A···N5	0.86	2.06	2.686(5)	128.8
N3–H3B···O1	0.86	1.99	2.592(5)	126.4
N3–H3B···O1^{vi}	0.86	2.24	3.039(5)	155.3
O5–H5A···N2^{ii}	0.830(19)	2.64(4)	3.286(5)	135(4)
O5–H5A···N4^{ii}	0.830(19)	2.08(3)	2.889(5)	164(5)
O5–H5B···O2^{vii}	0.842(19)	1.98(3)	2.772(5)	157(4)
O5–H5B···N1^{vii}	0.842(19)	2.69(2)	3.516(5)	168(5)
O3–H3C···N6^{viii}	0.843(19)	2.23(3)	3.028(5)	157(5)
O3–H3D···O5^{v}	0.868(19)	1.98(2)	2.801(6)	156(4)

Symmetry codes: (i) 1-x, -1-y, 2-z; (ii) 1-x, -y, 1-z; (iii) +x, -1+y, 1+z; (iv) +x, -1+y, +z; (v) -x, -y, 1-z; (vi) -x, 1-y, 2-z; (vii) -x, 1-y, 1-z; (viii) -1+x, 1+y, +z.

Table S2 Hydrogen bonds present in **2**

D–H···A	d(D–H)/Å	d(H–A)/Å	d(D–A)/Å	D–H–A/°
N3–H3A···N6^{i}	0.86	2.04	2.670(3)	129.4
N3–H3B···N5^{ix}	0.86	2.59	3.261(4)	135.9
N3–H3B···O2	0.86	1.95	2.580(3)	128.7
O1–H1A···N2^{x}	0.863(18)	1.97(2)	2.811(4)	166(3)
O1–H1B···N2^{xi}	0.831(18)	2.56(2)	3.344(4)	158(3)

symmetry codes: (i) 1-x, -y, 2-z; (ii) 1+x, +y, +z; (iii) 2-x, 1-y, 1-z; (iv) +x, -1+y, +z; (v) 1-x, 1-y, 2-z; (vi) -1+x, -1+y, 1+z; (vii) -x, -y, 2-z; (viii) -1+x, +y, +z; (ix) +x, 1+y, +z. (x) -1+x, 1+y, +z; (xi) 1-x, 1-y, 1-z.

Table S3 Selected bond lengths (Å) and angles (°) for **1** and **2**

EMOF **1**					
Na1-O2	2.457(4)	Na1-O5	2.398(4)	N4-C2	1.346(5)
Na1-N2	2.531(4)	Na1-O3	2.393(4)	N5-C2	1.347(6)
Na1-N1	2.901(4)	N2-N1	1.318(5)	N5-N6^{ii}	1.307(5)
Na1-O4^{i}	2.365(4)	N2-C1	1.378(6)	N3-C1	1.318(5)
Na1-O4	2.391(5)	N4-C1	1.324(5)	C2-N6	1.362(5)
O4-Na1-N2	80.76(13)	O5-Na1-O2	138.59(13)	N6^{ii}-N5-C2	120.1(3)
O4^{i}-Na1-N2	99.00(15)	O3-Na1-O2	83.89(13)	N4-C1-N2	109.7(4)
O4^{i}-Na1-O4	87.86(14)	O3-Na1-N2	87.85(14)	N3-C1-N2	124.7(4)
O4-Na1-O5	89.60(14)	O3-Na1-O5	90.41(14)	N4-C2-N5	124.4(4)
O4^{i}-Na1-O5	84.89(14)	N1-N2-C1	120.3(3)	N4-C2-N6	113.9(4)
O4-Na1-O3	104.66(15)	C1-N4-C2	124.1(4)	N5-C2-N6	121.7(4)
EMOF **2**					

Na1-N4^{iii}	2.601(3)	Na1-O3^{vi}	2.747(3)	N4-C1	1.327(4)
Na1-O1^{iv}	2.442(3)	N1-N2	1.317(3)	N4-C2	1.370(4)
Na1-O1	2.338(3)	N1-O2	1.265(3)	N5-N6	1.321(3)
Na1-O2	2.482(3)	N1-O3	1.256(3)	N5-C2	1.357(4)
Na1-O2^{v}	2.621(3)	N2-C1	1.398(4)	N6-C2^{vii}	1.357(4)
Na1-O3^{v}	2.623(3)	N3-C1	1.324(4)		
N4^{iii}-Na1-O2^{v}	100.22(9)	O2-Na1-O2^{v}	94.61(9)	N5-N6-C2^{vii}	119.3(2)
N4^{iii}-Na1-O3^{v}	147.59(9)	O2-Na1-O3^{v}	77.88(9)	Na1-O1-Na1^{v}	103.40(10)
O1^{iv}-Na1-N1^{v}	150.63(9)	O3^{v}-Na1-N1^{v}	24.75(7)	Na1-O2-Na1^{iv}	94.61(9)
O1-Na1-N1^{v}	93.35(9)	O3^{v}-Na1-O3^{vi}	67.11(8)	Na1^{iv}-O3-Na1^{vi}	112.89(8)
O1-Na1-N4^{iii}	84.47(9)	O2-N1-N2	125.7(2)	N3-C1-N2	123.6(3)
O1-Na1-O1^{iv}	103.40(10)	O3-N1-N2	116.3(2)	N3-C1-N4	126.1(3)
O1-Na1-O2	174.37(10)	O3-N1-O2	118.1(2)	N4-C1-N2	110.3(2)
O1-Na1-O3^{v}	96.74(10)	N1-N2-C1	120.4(2)	N5-C2-N4	113.6(2)
O2-Na1-N1^{v}	81.07(9)	C1-N4-C2	122.5(2)	N5-C2-N6^{vii}	122.3(3)
O2-Na1-N4^{iii}	99.17(9)	N6-N5-C2	118.4(2)	N6^{vii}-C2-N4	124.2(2)

symmetry codes: (i) 1-x, -y, 1-z; (ii) 1-x, -1-y, 2-z; (iii) +x, 1+y, +z; (iv) 1+x, +y, +z; (v) -1+x, +y, +z; (vi) 2-x, 1-y, 1-z; (vii) 1-x, -y, 2-z.

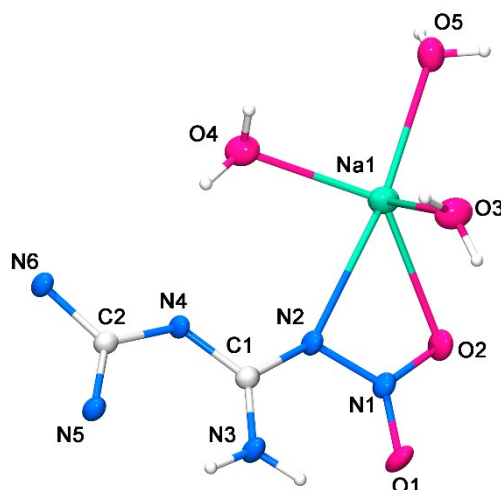## 2. Crystal structures and powder X-ray diffraction patterns for 1 and 2.

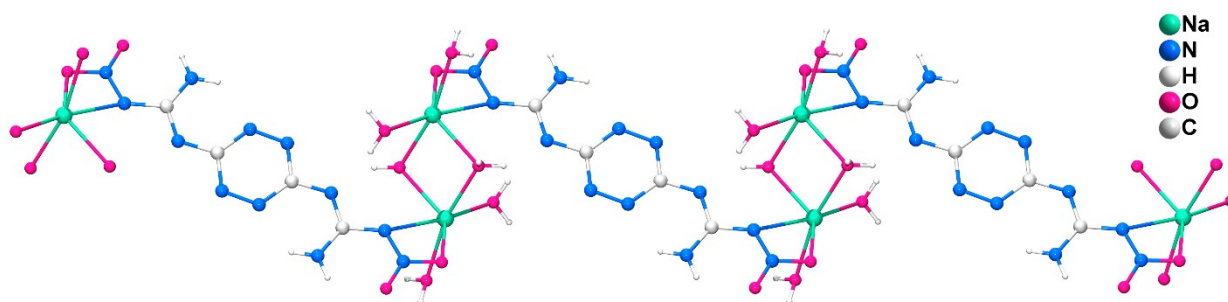**Fig. S1** The ellipsoid diagram of the asymmetric unit of **1**. Ellipsoids are at 30% probability.

Fig. S2 The 1D metal organic chain of **1** connected by Na cations and bridge water molecules.
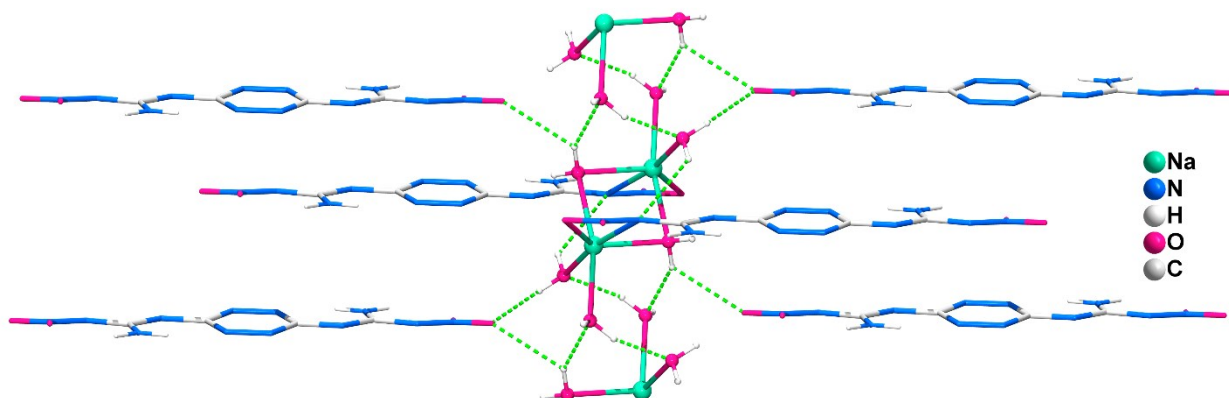

Fig. S3 The hydrogen-bonding network around the coordinate water molecules in **1**. Hydrogen bonds are shown as green dash lines.
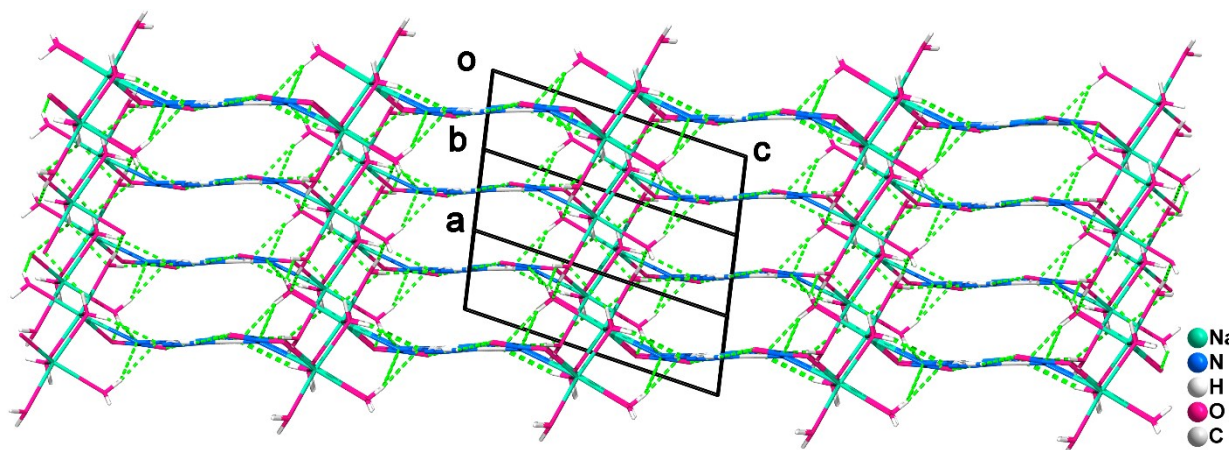

Fig. S4 The 3D layered hydrogen-bonding network of **1**. Hydrogen bonds are shown as green dash lines.
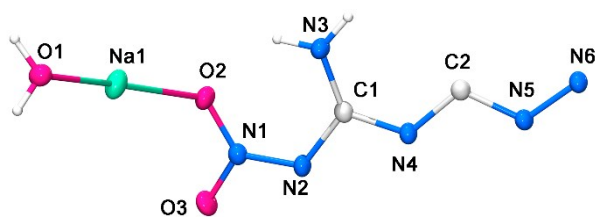

Fig. S5 The ellipsoid diagram of the asymmetric unit of **2**. Ellipsoids are at 30% probability.
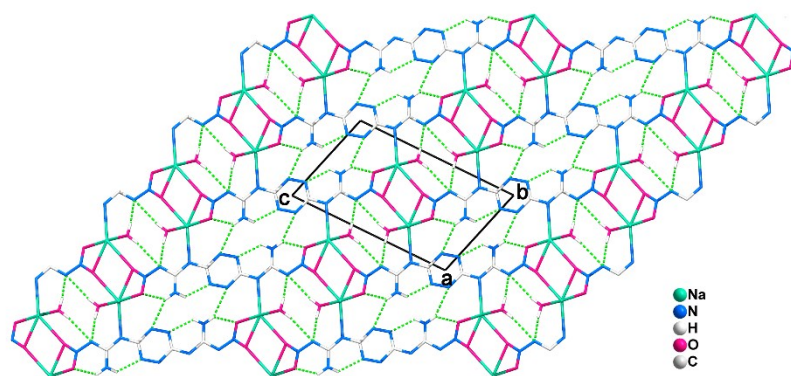
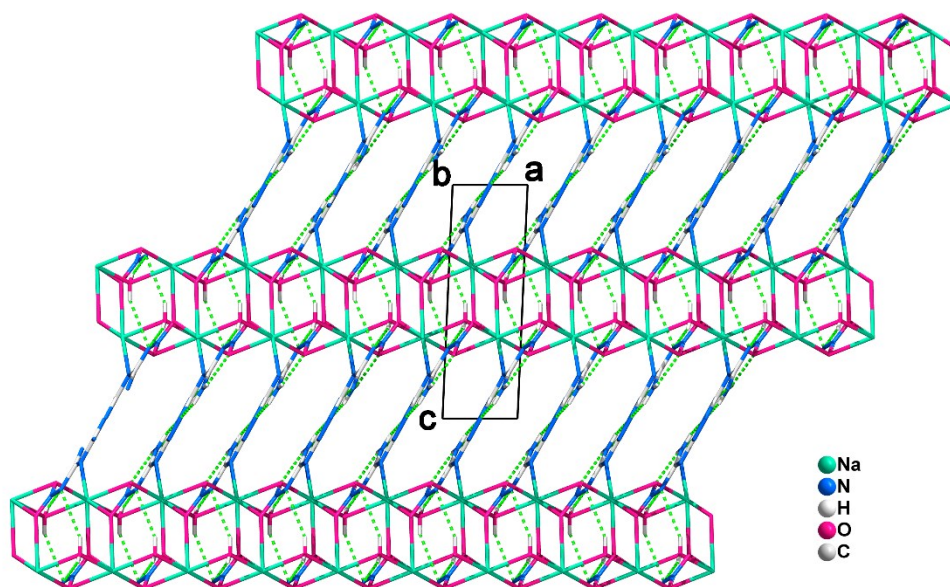**Fig. S6** The 3D structure of **2** viewing along *a* axis. Hydrogen bonds are shown as green dash lines.

Fig. S7 The 3D structure of **2** viewing along *b* axis. Hydrogen bonds are shown as green dash lines.
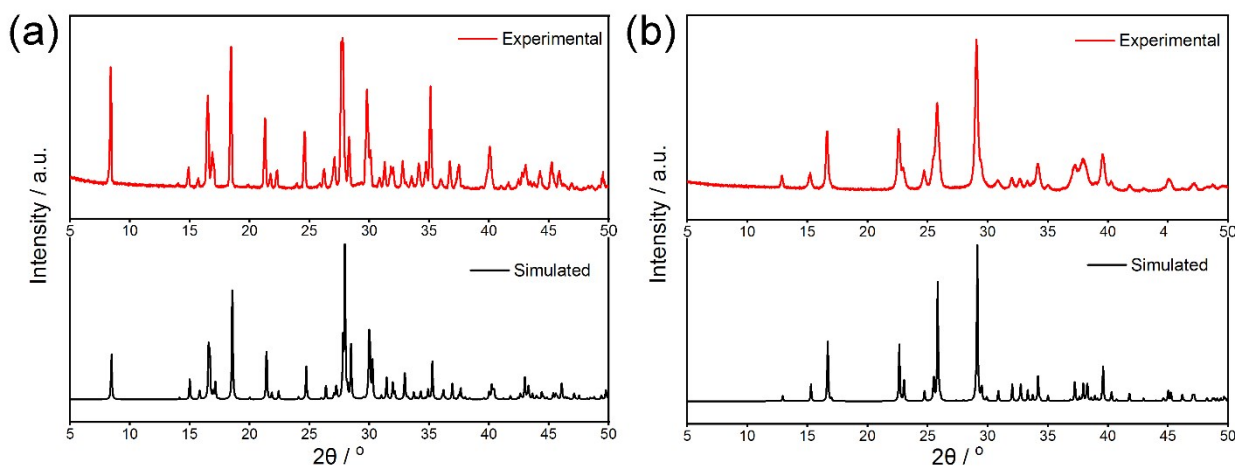
Fig. S8 The experimental and simulated powder X-ray diffraction patterns for **1** (a) and **2** (b).

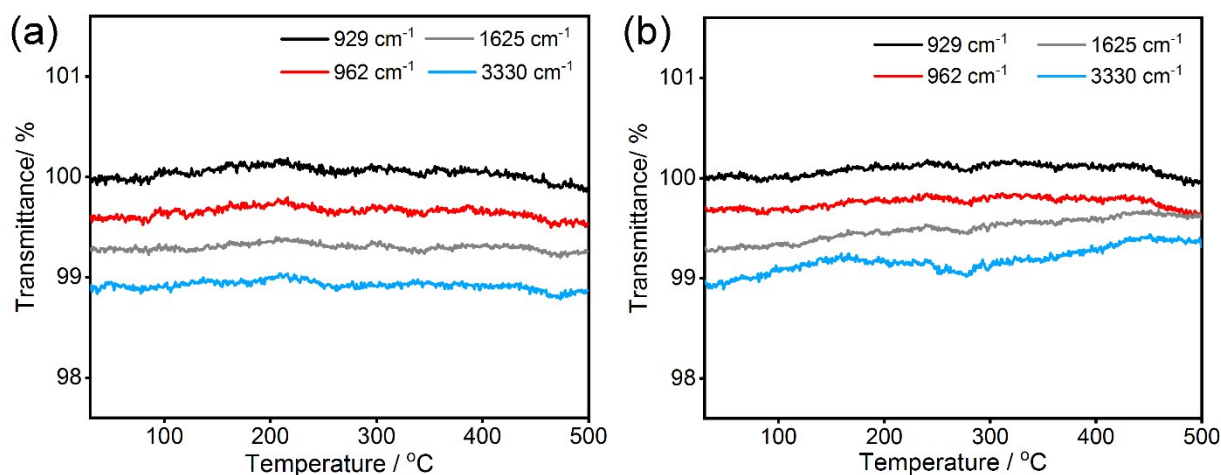## 3. Infrared spectra of simultaneous analysis.

Fig. S9 The infrared transmittance of characteristic absorption peaks of NH_3 for **1** (a) and **2** (b).

4. Computational details.

Gaussian 16 program (Revision C.01) was chosen to carry out the theoretical calculations.[1] Geometric optimization and frequency analyses were carried out using B3LYP/6-31+G* and the single-point energies were calculated by MP2/6-311++G** level.[2] The heat of formation (HOF) for DNGTz anion were determined using isodesmic reactions (Scheme S1) while the

heat of formation for other compounds were obtained by using G2 ab initio method based on atomization reaction and NIST WebBook.[3,4] The calculation results were list in Table S4. The optimized structure and XYZ coordinates of DNGTz anion are given in Fig. S10 and Table S5.
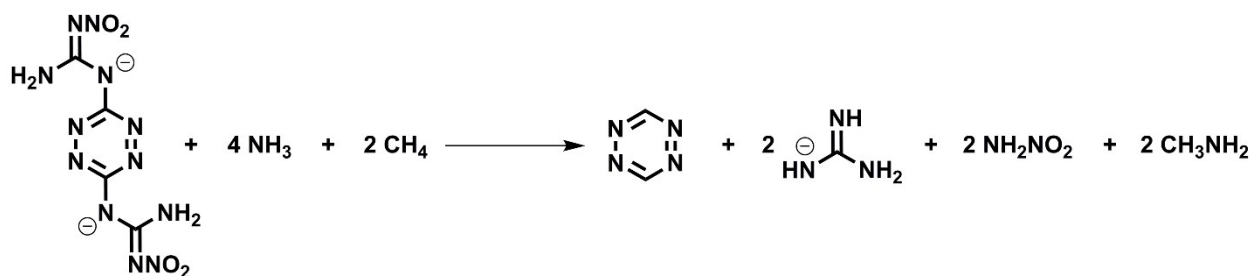

Scheme S1 The isodesmic reaction that used to calculate the heat of formation of DNGTz anion.

Table S4 The calculated HOF of the gas-phase species

Compounds	ΔH_f° (kJ·mol^{-1})
$C_2H_2N_4$	483.01
$CH_4N_3^-$	56.17
NH_2NO_2	3.12
CH_3NH_2	-23.50
NH_3	-45.94
CH_4	-74.87
DNGTz^{2-}	354.77
Na$^+$	585.00[a]

[a] From literature 5.

Meanwhile, the solid-phase heat of formation is calculated on the basis of Born-Haber energy cycle, which is shown in Scheme S2. The calculation equation is simplified by using equation 1.
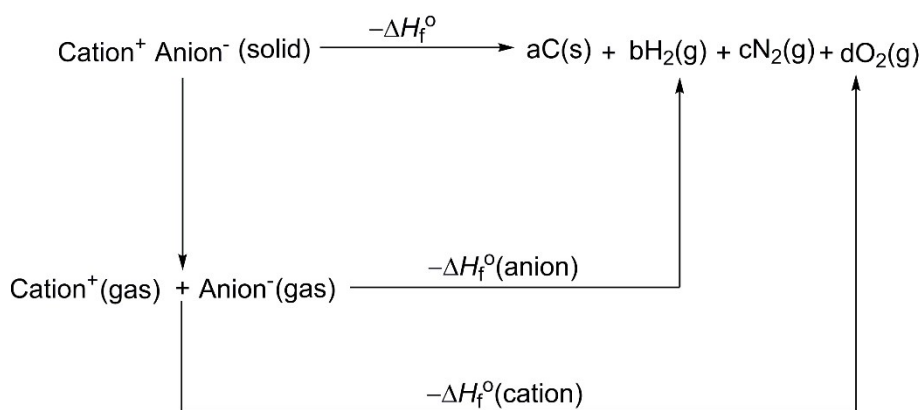
Scheme S2 Born-Haber energy cycle for the formation of **1** and **2**.

$$\Delta H_f^o(salt, 298\ K) = \Delta H_f^o(cation, 298\ K) + \Delta H_f^o(anion, 298\ K) - \Delta H_L \quad (1)$$

where ΔH_L represents the lattice energy of the ionic salts and it can be obtained by using the formula suggested by Jenkins, et al (equation 2).[6]

$$\Delta H_L = U_{pot} + [p\left(\frac{n_M}{2} - 2\right) + q(\frac{n_X}{2} - 2)]RT \quad (2)$$

where n_M and n_X depend on the nature of the ions, M^{q+} and M^{q+}, and are equal to 3 for monatomic ions, 5 for linear polyatomic ions, and 6 for nonlinear polyatomic ions. In equation 2, U_{pot} denotes the lattice potential energy that can be calculated from equation 3:

$$U_{pot}(kJ \cdot mol^{-1}) = \gamma(\rho_m/M_m)^{1/3} + \delta \quad (3)$$

In this equation, ρ_m represents the density of the salt and M_m equals to the chemical formula mass of the ionic material. Besides, the values of coefficients $\gamma(kJ \cdot mol^{-1} \cdot cm)$ and $\delta(kJ \cdot mol^{-1})$ can be assigned from the literature.[6]
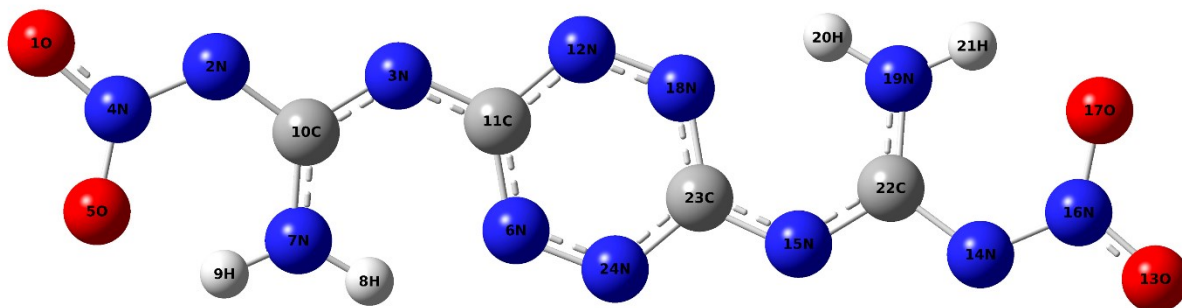
Fig. S10 The optimized structure of DNGTz anion.

Table S5 The XYZ coordinates of optimized structure of DNGTz anion

Center Number	Atomic Number	Forces (Hartrees/Bohr)		
		X	Y	Z
1	8	0.000000098	0.000000877	0.000000017
2	7	0.000000028	0.000000544	0.000000023
3	7	0.000000128	0.000000310	-0.000000002
4	7	0.000000103	0.000000752	-0.000000006
5	8	-0.000000143	0.000000719	0.000000008
6	7	-0.000000082	0.000000092	0.000000006
7	7	-0.000000157	0.000000480	-0.000000017
8	1	-0.000000215	0.000000319	0.000000026
9	1	-0.000000196	0.000000537	-0.000000003
10	6	-0.000000018	0.000000398	0.000000016
11	6	0.000000018	0.000000197	-0.000000001
12	7	0.000000158	0.000000026	-0.000000006
13	8	-0.000000109	-0.000000847	-0.000000007
14	7	-0.000000129	-0.000000552	-0.000000032
15	7	-0.000000150	-0.000000319	-0.000000014
16	7	-0.000000013	-0.000000709	0.000000011
17	8	0.000000141	-0.000000780	-0.000000019
18	7	0.000000105	-0.000000097	0.000000005
19	7	0.000000145	-0.000000460	-0.000000041
20	1	0.000000218	-0.000000287	0.000000019
21	1	0.000000180	-0.000000495	-0.000000023
22	6	0.000000059	-0.000000486	0.000000052
23	6	0.000000037	-0.000000180	0.000000002
24	7	-0.000000206	-0.000000037	-0.000000012

5. References.

1   M. J. Frisch, G. W. Trucks, H. B. Schlegel, G. E. Scuseria, M. A. Robb, J. R. Cheeseman, G. Scalmani, V. Barone, G. A. Petersson, H. Nakatsuji, X. Li, M. Caricato, A. V. Marenich, J. Bloino, B. G. Janesko, R. Gomperts, B. Mennucci, H. P. Hratchian, J. V. Ortiz, A. F. Izmaylov, J. L. Sonnenberg, Y. D. Williams, F. Ding, F. Lipparini, F. Egidi, J. Goings, B. Peng, A. Petrone, T. Henderson, D. Ranasinghe, V. G. Zakrzewski, J. Gao, N. Rega, G. Zheng, W. Liang, M. Hada, M. Ehara, K. Toyota, R. Fukuda, J. Hasegawa, M. Ishida, T. Nakajima, Y. Honda, O. Kitao, H. Nakai, T. Vreven, K. Throssell, J. A., Jr. Montgomery, J. E. Peralta, F. Ogliaro, M. J. Bearpark, J. J. Heyd, E. N. Brothers, K. N. Kudin, V. N. Staroverov, T. A. Keith, R. Kobayashi, J. Normand, K. Raghavachari, A. P. Rendell, J. C. Burant, S. S. Iyengar, J. Tomasi, M. Cossi, J. M. Millam, M. Klene, C. Adamo, R. Cammi, J. W. Ochterski, R. L. Martin, K. Morokuma, O. Farkas, J. B. Foresman and D. J. Fox, Gaussian 16, Revision C.01, Gaussian, Inc., Wallingford CT, 2016.

2   R. G. Parr and W. Yang, *Density Functional Theory of Atoms and Molecules*, Oxford University Press: Oxford, U.K., 1989.

3   L. A. Curtiss, K. Raghavachari, G. W. Trucks and J. A. Pople, *J. Chem. Phys.*, 1991, **94**, 7221- 7230.

4   NIST Chemistry WebBook, https://webbook.nist.gov/chemistry/, (accessed April 2020).

5   H. Gao, C. Ye, C. M. Piekarski and J. M. Shreeve, *J. Phys. Chem. C*, 2007, **111**, 10718-10731.

6   H. D. B. Jenkins, D. Tudela and L. Glasser, *Inorg. Chem.*, 2002, **41**, 2364-2367.